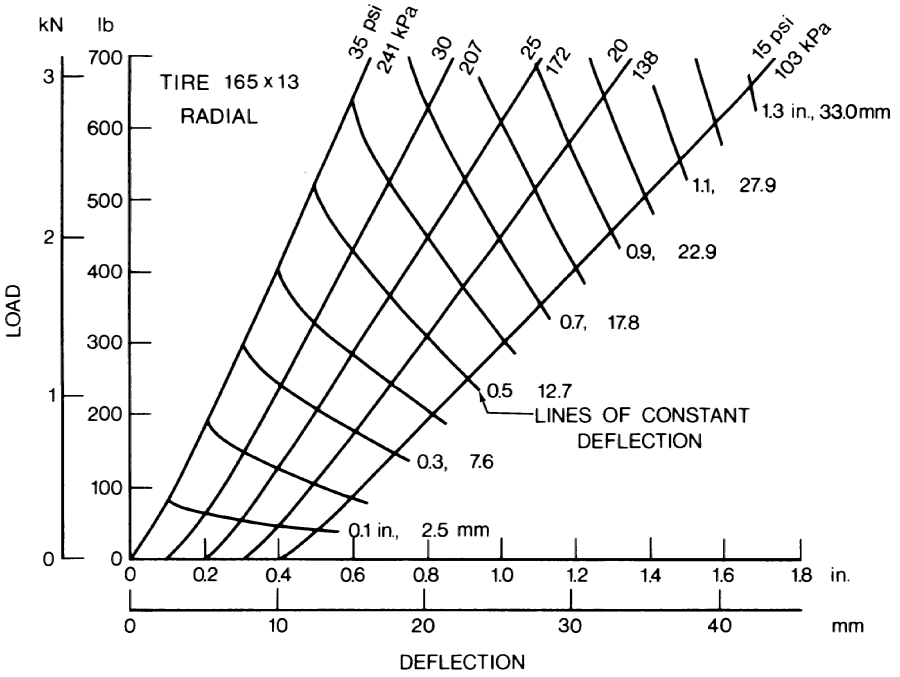

Fig. 1.54 Static load–deflection relationship of a radial-ply car tire. (Reproduced with permission of the Council of the Institution of Mechanical Engineers from reference 1.35.)

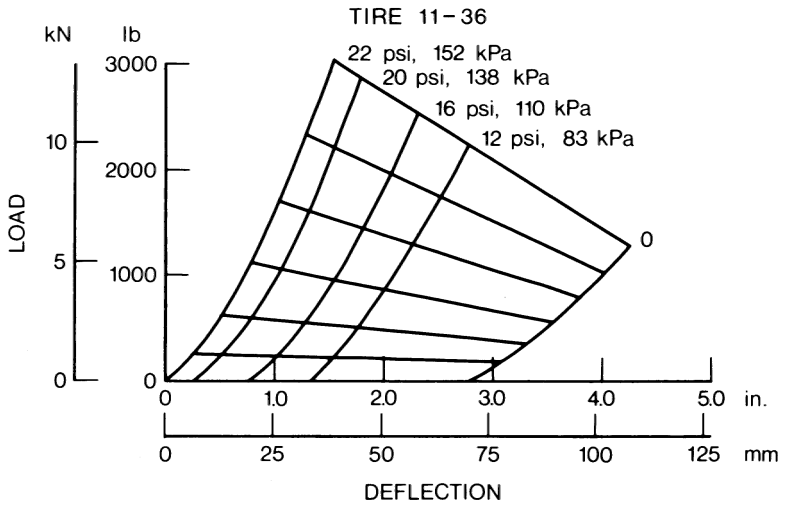

Fig. 1.55 Static load–deflection relationship of a tractor tire 11–36. (Reproduced with permission of the *Journal of Agricultural Engineering Research* from reference 1.36.)

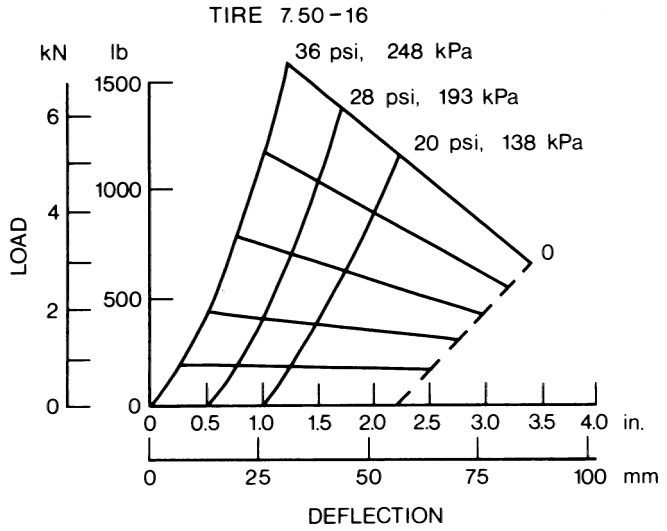

Fig. 1.56 Static load–deflection relationship of a tractor tire 7.50–16. (Reproduced with permission of the *Journal of Agricultural Engineering Research* from reference 1.36.)

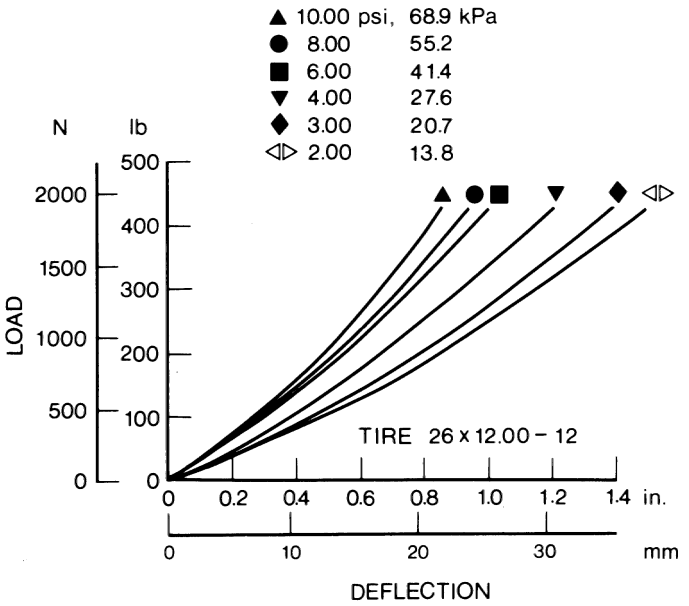

Fig. 1.57 Static load–deflection relationship of a terra tire 26 × 12.00–12 for all-terrain vehicles.

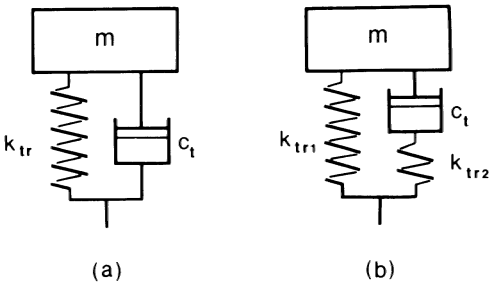

Fig. 1.58 (a) A linear model and (b) a viscoelastic model for tire vibration analysis.

response of the tire is recorded. A typical amplitude decay trace is shown in Fig. 1.60. The values of the equivalent viscous damping coefficient c_{eq} and the dynamic stiffness k_z of the tire can then be determined from the decay trace using the well-established theory of free vibration for a single-degree-of-freedom system:

$$c_{eq} = \sqrt{\frac{4m^2\omega_d^2\delta^2/(\delta^2 + 4\pi^2)}{1 - [\delta^2/(\delta^2 + 4\pi^2)]}} \tag{1.91}$$

and

$$k_z = \frac{m\omega_d^2}{1 - \delta^2/(\delta^2 + 4\pi^2)} \tag{1.92}$$

ω_d is the damped natural frequency of the tire with mass m, and can be identified from the amplitude decay trace shown in Fig. 1.60.

$$\omega_d = 2\pi/\tau \tag{1.93}$$

where τ is the period of damped oscillation shown in Fig. 1.60.

δ is the logarithmic decrement, which is defined as the natural logarithm of the ratio of any two successive amplitudes, such as x_1 and x_2, shown in Fig. 1.60.

$$\delta = \ln (x_1/x_2) \tag{1.94}$$

The drop test may also be performed utilizing a tire endurance testing machine consisting of a beam pivoted at one end, which carries the test tire loaded against a drum. To initiate the test, the beam is displaced and the system is set in angular oscillation about the pivot of the beam. A decay trace for the amplitude of angular displacement is recorded. A set of equations for

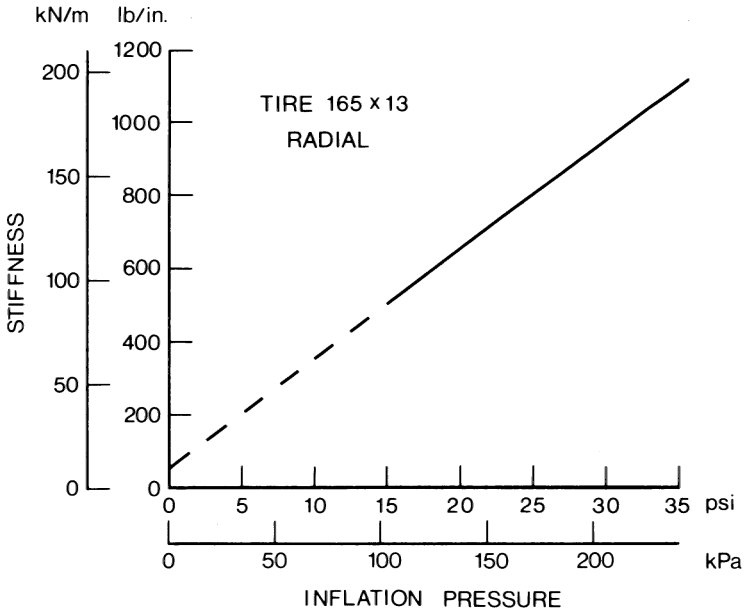

Fig. 1.59 Variation of static stiffness with inflation pressure for a radial-ply car tire. (Reproduced with permission of the Council of the Institution of Mechanical Engineers from reference 1.35.)

this torsional system, similar to that for a single-degree-of-freedom linear system described above, can be derived for determining the equivalent damping coefficient and nonrolling dynamic stiffness for the tire from the decay trace.

Table 1.9 shows the values of the nonrolling dynamic stiffness and the damping coefficient for the tractor tires 11–36 and 7.5–16 [1.36], and the damping coefficient for the terra tire 26 × 12.00–12. The values of the damping coefficient for the 5.60 × 13 bias-ply and the 165 × 13 radial-ply car tire are given in Table 1.10 [1.35].

Rolling Dynamic Stiffness The rolling dynamic stiffness is usually determined by measuring the response of a rolling tire to a known harmonic excitation. The response is normally measured at the hub, and the excitation is given at the tread. By examining the ratio of output to input and the phase angle, it is possible to determine the dynamic stiffness and the damping coefficient of a rolling tire.

An alternative method for determining the dynamic stiffness of a tire is to measure its resonant frequency when rolling on a drum or belt. Figure 1.61 shows the values of the dynamic stiffness for various types of car tire obtained using this method [1.6]. It is shown that the dynamic stiffness of car tires

TABLE 1.9 Vertical Stiffness of Tires

Tire	Inflation Pressure	Load	Static Stiffness	Nonrolling Dynamic Stiffness (Average)	Damping Coefficient
11–36	82.7 kPa	6.67 kN (1500 lb)	357.5 kN/m (24,500 lb/ft)	379.4 kN/m (26,000 lb/ft)	2.4 kN · s/m (165 lb · s/ft)
(4-ply)	(12 psi)	8.0 kN (1800 lb)	357.5 kN/m (24,500 lb/ft)	394.0 kN/m (27,000 lb/ft)	2.6 kN · s/m (180 lb · s/ft)
		9.34 kN (2100 lb)	—	423.2 kN/m (29,000 lb/ft)	3.4 kN · s/m (230 lb · s/ft)
	110.3 kPa	6.67 kN (1500 lb)	379.4 kN/m (26,000 lb/ft)	394.0 kN/m (27,000 lb/ft)	2.1 kN · s/m (145 lb · s/ft)
	(16 psi)	8.0 kN (1800 lb)	386.7 kN/m (26,500 lb/ft)	437.8 kN/m (30,000 lb/ft)	2.5 kN · s/m (175 lb · s/ft)
		9.34 kN (2100 lb)	394.0 kN/m (27.000 lb/ft)	423.2 kN/m (29,000 lb/ft)	2.5 kN · s/m (175 lb · s/ft)
7.5–16	138 kPa	3.56 kN (800 lb)	175.1 kN/m (12,000 lb/ft)	218.9 kN/m (15,000 lb/ft)	0.58 kN · s/m (40 lb · s/ft)
(6-ply)	(20 psi)	4.45 kN (1000 lb)	175.1 kN/m (12,000 lb/ft)	233.5 kN/m (16,000 lb/ft)	0.66 kN · s/m (45 lb · s/ft)
		4.89 kN (1100 lb)	182.4 kN/m (12,500 lb/ft)	248.1 kN/m (17,000 lb/ft)	0.80 kN · s/m (55 lb · s/ft)
	193 kPa	3.56 kN (800 lb)	218.9 kN/m (15,000 lb/ft)	233.5 kN/m (16,000 lb/ft)	0.36 kN · s/m (25 lb · s/ft)
	(28 psi)	4.45 kN (1100 lb)	226.2 kN/m (15,500 lb/ft)	262.7 kN/m (18,000 lb/ft)	0.66 kN · s/m (45 lb · s/ft)
		4.89 kN (1300 lb)	255.4 kN/m (17,500 lb/ft)	277.3 kN/m (19,000 lb/ft)	0.73 kN · s/m (50 lb · s/ft)
26 × 12.00–12	15.5 kPa	1.78 kN (400 lb)	51.1 kN/m (3500 lb/ft)	—	0.47 kN · s/m (32 lb · s/ft)
(2-ply)	(2.25 psi)				
	27.6 kPa	1.78 kN (400 lb)	68.6 kN/m (4700 lb/ft)	—	0.49 kN · s/m (34 lb · s/ft)
	(4 psi)				

Source: Reference 1.36

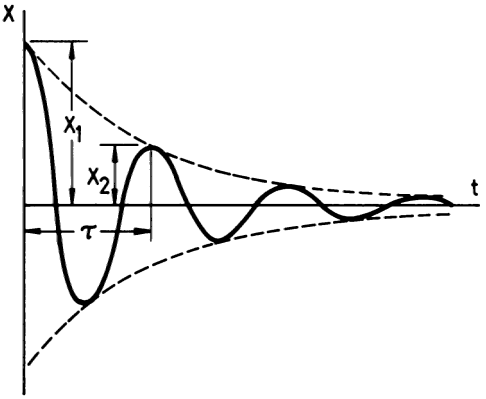

Fig. 1.60 An amplitude decay record of a nonrolling tire obtained from a drop test.

decreases sharply as soon as the tire is rolling. However, beyond a speed of approximately 20 km/h (12 mph), the influence of speed becomes less important.

Table 1.11 shows the values of vertical stiffness of a sample of truck tires at rated loads and inflation pressures [1.19]. They were obtained when the tires were rolling at a relatively low speed.

It can be seen from Table 1.11 that values of the vertical stiffness for the truck tires tested range from 764 to 1024 kN/m (4363 to 5850 lb/in.), and that the vertical stiffness of radial-ply truck tires is generally lower than that of bias-ply tires of similar size.

Figure 1.62 shows the variation of the dynamic stiffness of a 13.6 × 38 radial tractor tire with speed [1.37]. The static load on the tire was 18.25 kN (4092 lb), and the inflation pressure was 138 kPa (20 psi). It can be seen that the dynamic stiffness of the tractor tire decreases sharply as soon as the tire begins rolling, similar to that for passenger car tires shown in Fig. 1.61. The

TABLE 1.10 Damping Coefficient of Tires

Tire	Inflation Pressure	Damping Coefficient
Bias-ply	103.4 kPa (15 psi)	4.59 kN · s/m (315 lb · s/ft)
5.60 × 13	137.9 kPa (20 psi)	4.89 kN · s/m (335 lb · s/ft)
	172.4 kPa (25 psi)	4.52 kN · s/m (310 lb · s/ft)
	206.9 kPa (30 psi)	4.09 kN · s/m (280 lb · s/ft)
	241.3 kPa (35 psi)	4.09 kN · s/m (280 lb · s/ft)
Radial-ply	103.4 kPa (15 psi)	4.45 kN · s/m (305 lb · s/ft)
165 × 13	137.9 kPa (20 psi)	3.68 kN · s/m (252 lb · s/ft)
	172.4 kPa (25 psi)	3.44 kN · s/m (236 lb · s/ft)
	206.9 kPa (30 psi)	3.43 kN · s/m (235 lb · s/ft)
	241.3 kPa (35 psi)	2.86 kN · s/m (196 lb · s/ft)

Source: Reference 1.35.

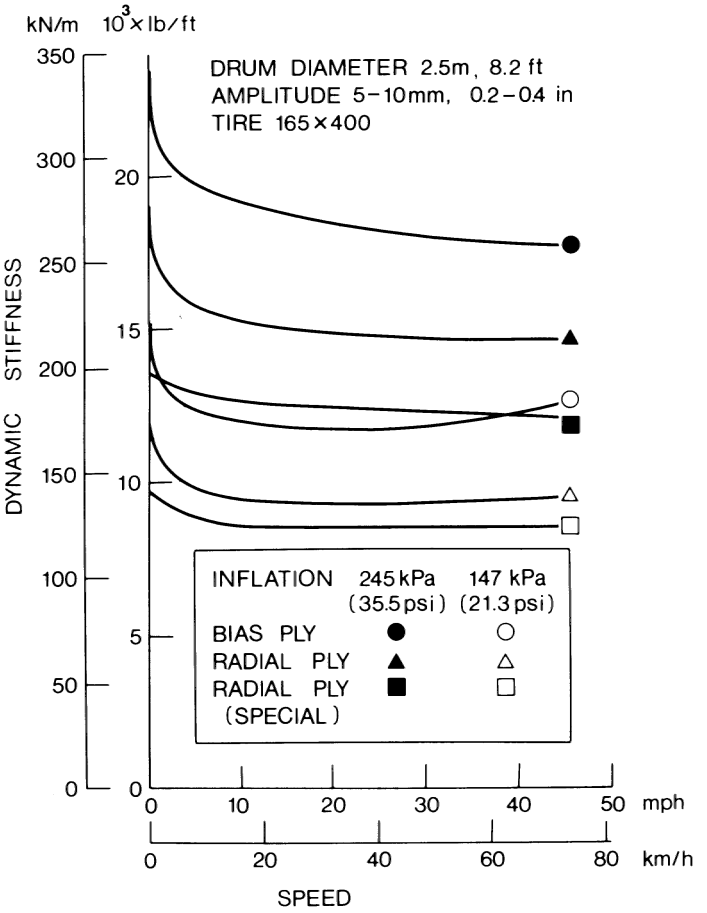

Fig. 1.61 Effect of speed on rolling dynamic stiffness of car tires. (Reproduced with permission from *Mechanics of Pneumatic Tires,* edited by S.K. Clark, Monograph 122, National Bureau of Standards, 1971.)

effects of inflation pressure on the dynamic stiffness of the same tire are shown in Fig. 1.63. The variation of the damping coefficient with speed for the tractor tire is shown in Fig. 1.64. It can be seen that beyond a speed of 1 km/h (0.6 mph), the damping coefficient drops rapidly until a speed of 5 km/h (3.1 mph) is reached, and then approaches an asymptote. The effects of inflation pressure on the damping coefficient are shown in Fig. 1.65.

Attempts to determine the relationship between the static and dynamic stiffness of tires have been made. However, no general conclusions have been reached. Some reports indicate that for passenger car tires, the rolling dynamic stiffness may be 10–15% less than the stiffness derived from static load–deflection curves, whereas for heavy truck tires, the dynamic stiffness is ap-

TABLE 1.11 Vertical Stiffness of Truck Tires at Rated Loads and Inflation Pressures

Tire Type	Tire Construction	Vertical Stiffness kN/m	Vertical Stiffness lb/in.
Unspecified 11.00-22/G	Bias-ply	1024	5850
Unspecified 11.00-22/F	Bias-ply	977	5578
Unspecified 15.00 × 22.5/H	Bias-ply	949	5420
Unspecified 11.00-20/F	Bias-ply	881	5032
Michelin Radial 11R22.5 XZA (1/3 Tread)	Radial-ply	874	4992
Michelin Radial 11R22.5 XZA (1/2 Tread)	Radial-ply	864	4935
Michelin Radial 11R22.5 XZA	Radial-ply	831	4744
Unspecified 10.00-20/F	Bias-ply	823	4700
Michelin Radial 11R22.5 XZA	Radial-ply	809	4622
Michelin Pilote 11/80R22.5 XZA	Radial-ply	808	4614
Unspecified 10.00-20/F	Bias-ply	788	4500
Michelin Pilote 11/80R22.5 XZA	Radial-ply	774	4418
Unspecified 10.00-20/G	Bias-ply	764	4363

Source: UMTRI, reference 1.19.

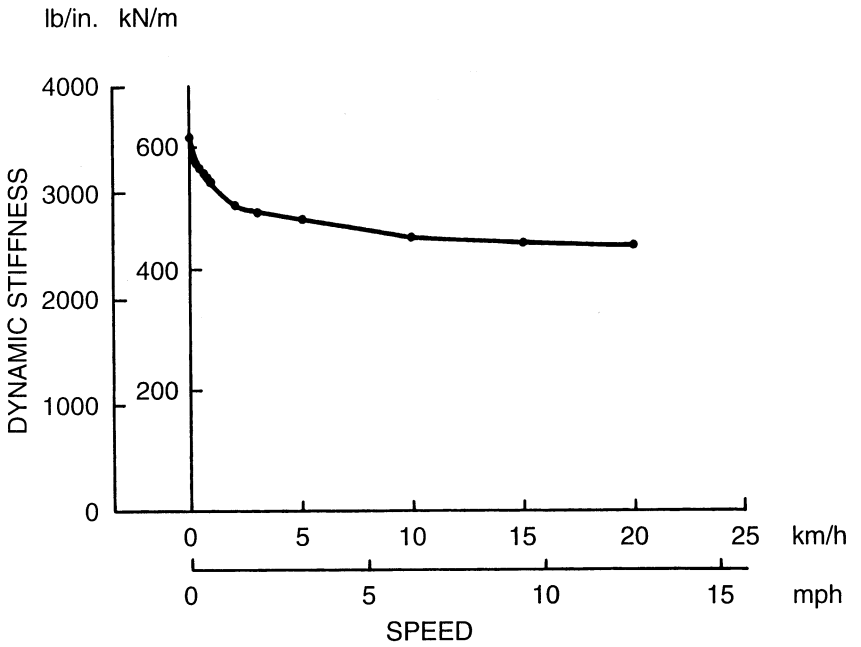

Fig. 1.62 Effect of speed on rolling dynamic stiffness of a radial-ply tractor tire 13.6 × 38. (Reproduced with permission from reference 1.37.)

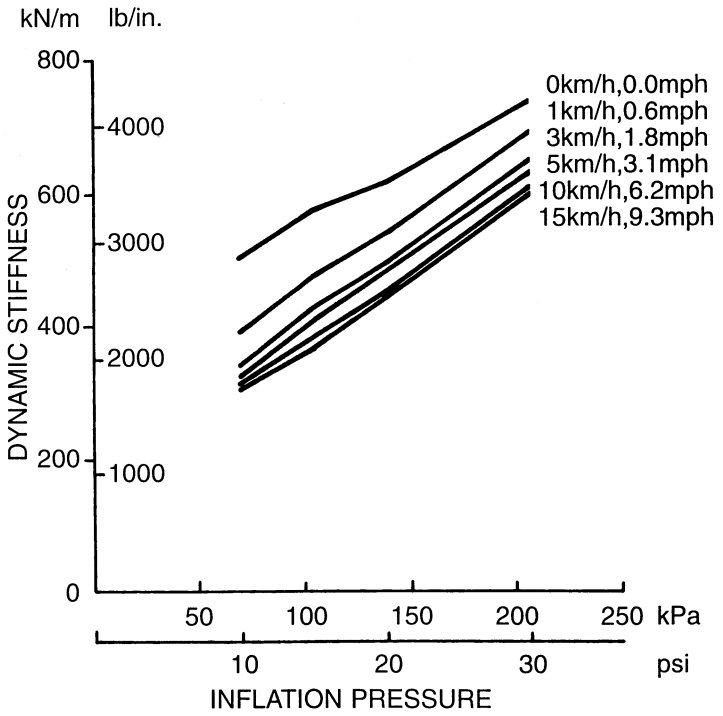

Fig. 1.63 Effect of inflation pressure on rolling dynamic stiffness at various speeds of a radial-ply tractor tire 13.6 × 38. (Reproduced with permission from reference 1.37.)

proximately 5% less than the static value. For tractor tires, it has been reported that the dynamic stiffness may be 26% lower than the static value. In simulation studies of vehicle ride, the use of the rolling dynamic stiffness is preferred.

It has been shown that among various operation parameters, inflation pressure, speed, normal load, and wear have a noticeable influence on tire stiffness. Tire design parameters, such as the crown angle of the cords, tread width, tread depth, number of plies, and tire material, also affect the stiffness.

The damping of a pneumatic tire is mainly due to the hysteresis of tire materials. Generally speaking, it is neither Coulomb-type nor viscous-type damping, and it appears to be a combination of both. However, an equivalent viscous damping coefficient can usually be derived from the dynamic tests mentioned previously. Its value is subject to variation, depending on the design and construction of the tire, as well as operating conditions. It has been shown that the damping of pneumatic tires made of synthetic rubber compounds is considerably less than that provided by a shock absorber.

To evaluate the overall vibrational characteristics of tires, tests may be carried out on a variable-speed rotating drum. The profile of the drum may

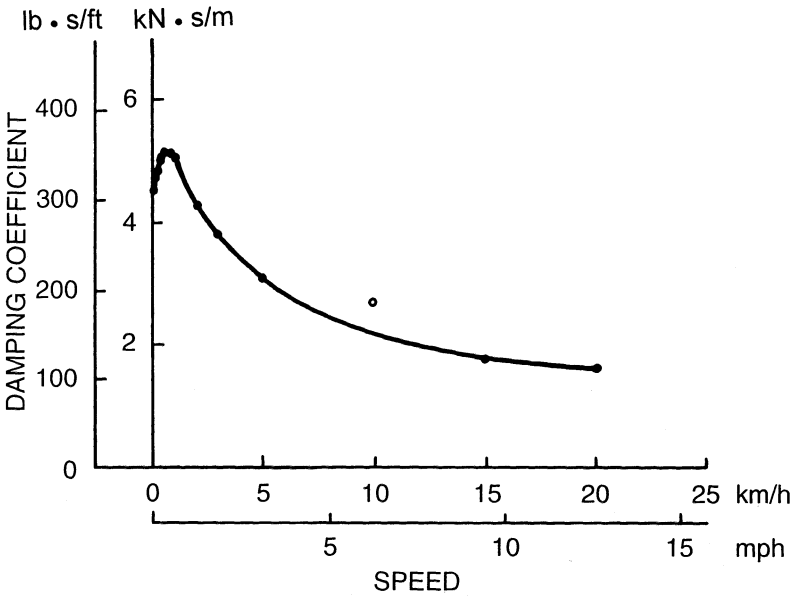

Fig. 1.64 Effect of speed on damping coefficient of a radial-ply tractor tire 13.6 × 38. (Reproduced with permission from reference 1.37.)

be random, sinusoidal, square, or triangular. Experience has shown that the use of a periodic type of excitation enables rapid assessments to be made. Figure 1.66 shows the wheel hub acceleration as a function of frequency for a radial-ply and a bias-ply tire over a sinusoidal profile with 133 mm (5.25 in.) pitch and 6 mm (0.25 in.) peak-to-peak amplitude [1.38]. The transmissibility ratios in the vertical direction over a wide frequency range of a radial-ply and a bias-ply tire are shown in Fig. 1.67 [1.38]. This set of results has been obtained using a vibration exciter. The vibration input is imparted to the tread of a nonrolling tire through a platform mounted on the vibration exciter.

It can be seen from Figs. 1.66 and 1.67 that the transmissibility ratio for vertical excitation of the radial-ply tire is noticeably higher than that of the bias-ply tire in the frequency range of 60–100 Hz. Vibrations in this frequency range contribute to the passenger's sensation of "harshness." On the other hand, the bias-ply tire is significantly worse than the radial-ply tire in the frequency range approximately 150–200 Hz. In this frequency range, vibrations contribute to induced tire noise, commonly known as "road roar" [1.1].

Tire noise is generated by the following major mechanisms [1.23]:

1) Air pumping effect—As the tire rolls, air is trapped and compressed in the voids between the tread and the pavement. Noise is generated when the compressed air is released at high speed to the atmosphere at the exit of the contact patch.

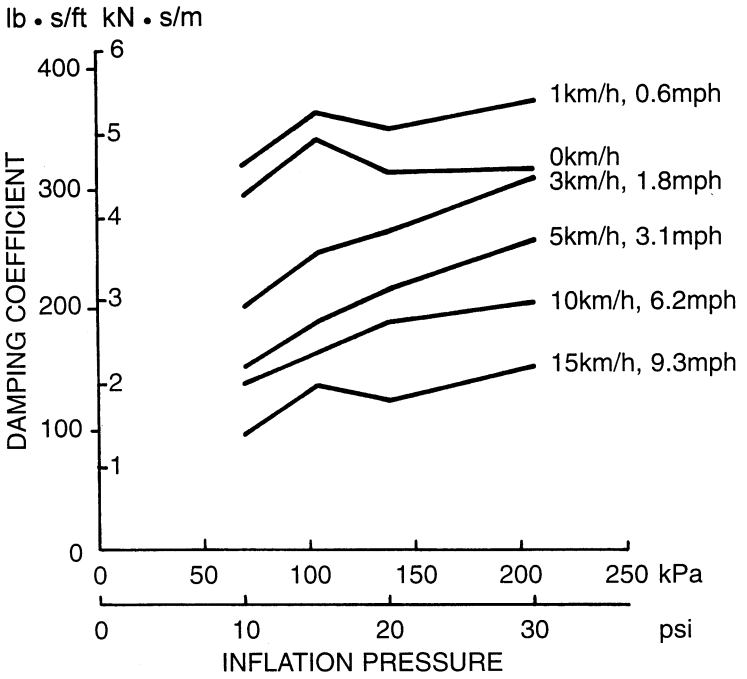

Fig. 1.65 Effect of inflation pressure on damping coefficient at various speeds of a radial-ply tractor tire 13.6 × 38. (Reproduced with permission from reference 1.37.)

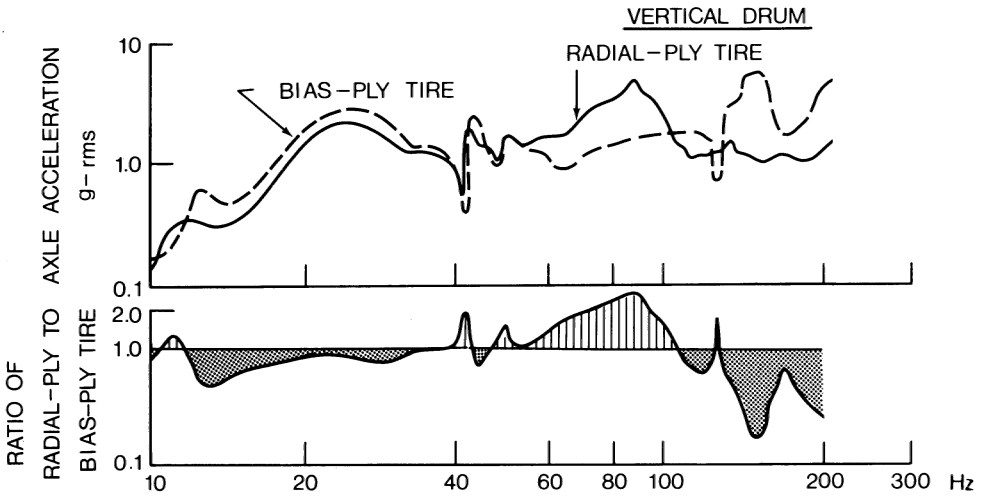

Fig. 1.66 Vibration characteristics of a bias-ply and a radial-ply car tire subject to sinusoidal excitation. (Reproduced with permission of the Council of the Institution of Mechanical Engineers from reference 1.38.)

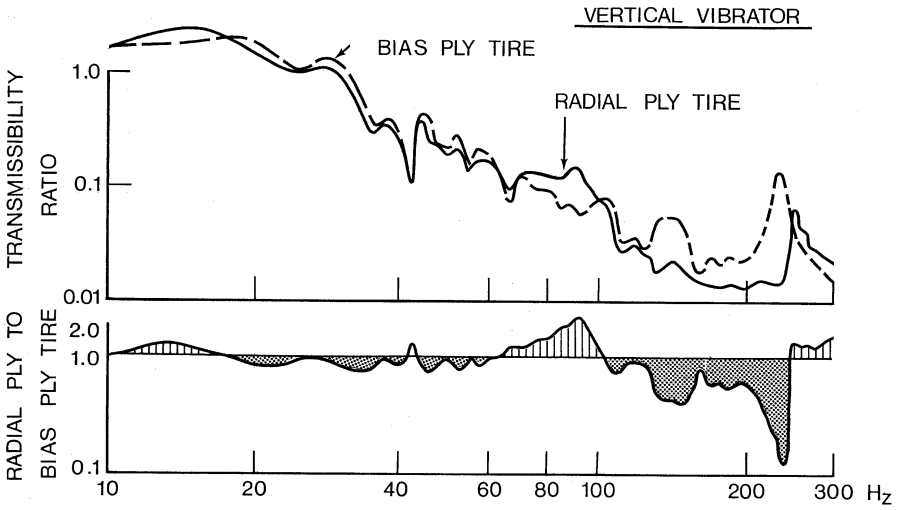

Fig. 1.67 Transmissibility ratio of a bias-ply and a radial-ply car tire. (Reproduced with permission of the Council of the Institution of Mechanical Engineers from reference 1.38.)

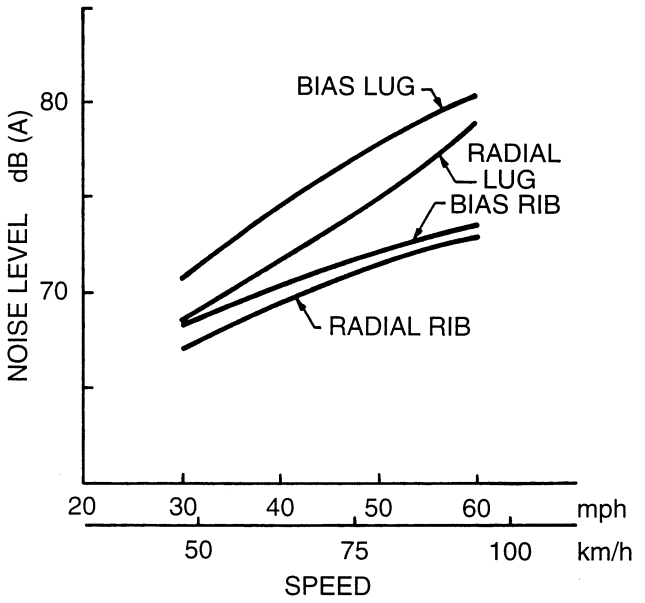

Fig. 1.68 Effect of speed on noise generated by bias-ply and radial-ply truck tires. (Reproduced with permission of the Society of Automotive Engineers from reference 1.23.)

TABLE 1.12 Effect of Pavement Texture on Noise Level Generated by a Bias-Ply Truck Tire

Road Surface	Noise Level dB (A)
Moderately smooth concrete	70
Smooth asphalt	72
Worn concrete (exposed aggregate)	72
Brushed concrete	78

Source: Reference 1.23.

2) Tread element vibrations—Tread elements impact the pavement as the tire rolls. When the elements leave the contact patch, they are released from a highly stressed state. These induce vibrations of the tread, which form a major source of tire noise. Carcass vibrations and the grooves and lug voids in the tread acting like resonating pipes also contribute to noise radiation from the tire.

Since the air pumping effect, the vibrations of tread elements and carcass, etc., are related to speed, the noise level generated by a tire is a function of operating speed. Figure 1.68 shows the variations of noise level with speed for various types of truck tire on a smooth pavement [1.23]. The results were obtained following the SAE J57 test procedure.

The effect of pavement texture on the noise level generated by a bias-ply, ribbed truck tire at 80 km/h (50 mph) is shown in Table 1.12 [1.23].

REFERENCES

1.1 T. French, *Tire Technology.* Bristol and New York: Adam Hilger, 1989.

1.2 V.E. Gough, ''Structure of the Tire,'' in S.K. Clark, Ed., *Mechanics of Pneumatic Tires,* Monograph 122. Washington, DC: National Bureau of Standards, 1971.

1.3 D.F. Moore, *The Friction of Pneumatic Tyres.* Amsterdam: Elsevier, 1975.

1.4 *Vehicle Dynamics Terminology,* SAE J670e, Society of Automotive Engineers, 1978.

1.5 T. French, ''Construction and Behaviour Characteristics of Tyres,'' in *Proc. of the Institution of Mechanical Engineers, Automobile Division,* AD 14/59, 1959.

1.6 H.C.A. van Eldik and Thieme and H.B. Pacejka, ''The Tire as a Vehicle Component,'' in S.K. Clark, Ed., *Mechanics of Pneumatic Tires,* Monograph 122. Washington, DC: National Bureau of Standards, 1971.

1.7 *Automotive Handbook,* 2nd ed. Robert Bosch GmbH, 1986.

1.8 L. Segel, ''The Mechanics of Heavy-Duty Trucks and Truck Combinations,'' presented at the Engineering Summer Conferences, University of Michigan, Ann Arbor, 1984.

1.9 J.D. Hunt, J.D. Walter, and G.L. Hall, "The Effect of Tread Polymer Variations on Radial Tire Rolling Resistance," Society of Automotive Engineers, Special Publications, P-74, *Tire Rolling Losses and Fuel Economy—An R&D Planning Workshop,* 1977.

1.10 L.W. DeRaad, "The Influence of Road Surface Texture on Tire Rolling Resistance," Society of Automotive Engineers, Special Publication P-74, *Tire Rolling Losses and Fuel Economy—An R&D Planning Workshop,* 1977.

1.11 B.L. Collier and J.T. Warchol, "The Effect of Inflation Pressure on Bias, Bias-Belted and Radial Tire Performance," Society of Automotive Engineers, paper 800087, 1980.

1.12 J.J. Taborek, "Mechanics of Vehicles," *Machine Design,* May 30–Dec. 26, 1957.

1.13 J.D.C. Hartley and D.M. Turner, "Tires for High-Performance Cars," *SAE Transactions,* vol. 64, 1956.

1.14 M.L. Janssen and G.L. Hall, "Effect of Ambient Temperature on Radial Tire Rolling Resistance," Society of Automotive Engineers, paper 800090, 1980.

1.15 R. Hadekel, "The Mechanical Characteristics of Pneumatic Tyres," S&T Memo No. 10/52, Ministry of Supply, London, England, 1952.

1.16 P.S. Fancher and P. Grote, "Development of a Hybrid Simulation for Extreme Automobile Maneuvers," in *Proc. 1971 Summer Computer Simulation Conf.,* Boston, MA, 1971.

1.17 J.L. Harned, L.E. Johnston, and G. Sharpf, "Measurement of Tire Brake Force Characteristics as Related to Wheel Slip (Antilock) Control System Design," *SAE Transactions,* vol. 78, paper 690214, 1969.

1.18 R.D. Ervin, "Mobile Measurement of Truck Tire Traction," in *Proc. Symposium on Commercial Vehicle Braking and Handling,* Highway Safety Research Institute, University of Michigan, Ann Arbor, 1975.

1.19 P.S. Fancher, R.D. Ervin, C.B. Winkler, and T.D. Gillespie, "A Fact Book of the Mechanical Properties of the Components for Single-Unit and Articulated Heavy Trucks," Report No. DOT HS 807 125, National Highway Traffic Safety Administration, U.S. Department of Transportation, 1986.

1.20 V.E. Gough, "Practical Tire Research," *SAE Transactions,* vol. 64, 1956.

1.21 D.L. Nordeen and A.D. Cortese, "Force and Moment Characteristics of Rolling Tires," Society of Automotive Engineers, paper 713A, 1963.

1.22 J.R. Ellis, *Vehicle Handling Dynamics.* London: Mechanical Engineering Publications, 1994.

1.23 T.L. Ford and F.S. Charles, "Heavy Duty Truck Tire Engineering," *The Thirty-Fourth L. Ray Buckendale Lecture,* Society of Automotive Engineers, SP-729, 1988.

1.24 E. Bakker, L. Nyborg, and H.B. Pacejka, "Tyre Modelling for Use in Vehicle Dynamic Studies," Society of Automotive Engineers, paper 870421, 1987.

1.25 E. Bakker, H.B. Pacejka, and L. Lidner, "A New Tire Model with an Application in Vehicle Dynamic Studies," Society of Automotive Engineers, paper 890087, 1989.

1.26 H.B. Pacejka, "The Tyre as a Vehicle Component," in *Proc. XXVI FISITA Congress,* Prague, June 16–23, 1996 (CD-ROM).

1.27 H.B. Pacejka and I.J.M. Besselink, "Magic Formula Tyre Model with Transient Properties," in F. Bohm and H.-P. Willumeit, Eds., *Proc. 2nd Int. Colloquium on Tyre Models for Vehicle Dynamic Analysis,* Berlin. Lisse, The Netherlands: Swets & Zeitlinger, 1997.

1.28 P. Bayle, J.F. Forissier, and S. Lafon, "A New Tyre Model for Vehicle Dynamics Simulations," in *Automotive Technology International '93.* U.K. & International Press, 1993.

1.29 A. van Zanten, W.D. Ruf, and A. Lutz, "Measurement and Simulation of Transient Tire Forces," Society of Automotive Engineers, paper 890640, 1989.

1.30 J. Zhou, J.Y. Wong, and R.S. Sharp, "A Multi-Spoke, Three Plane Tyre Model for Simulation of Transient Behavior," *Vehicle System Dynamics,* vol. 31, no. 1, 1999.

1.31 A. Schallamach, "Skid Resistance and Directional Control," in S.K. Clark, Ed., *Mechanics of Pneumatic Tires,* Monograph 112. Washington, DC: National Bureau of Standards, 1971.

1.32 S.K. Clark, "The Contact Between Tire and Roadway," in S.K. Clark, Ed., *Mechanics of Pneumatic Tires,* Monograph 122. Washington, DC: National Bureau of Standards, 1971.

1.33 W.B. Horne and R.C. Dreher, "Phenomena of Pneumatic Tire Hydroplaning," NASA TND-2056, Nov. 1963.

1.34 W.B. Horne and U.T. Joyner, "Pneumatic Tire Hydroplaning and Some Effects on Vehicle Performance," Society of Automotive Engineers, paper 650145, 1965.

1.35 J.A. Overton, B. Mills, and C. Ashley, "The Vertical Response Characteristics of the Non-Rolling Tire," in *Proc. Institution of Mechanical Engineers,* vol. 184, part 2A, no. 2, 1969–1970.

1.36 J. Matthews and J.D.C. Talamo, "Ride Comfort for Tractor Operators, III. Investigation of Tractor Dynamics by Analogue Computer Simulation," *Journal of Agricultural Engineering Research,* vol. 10, no. 2, 1965.

1.37 J.A. Lines and N.A. Young, "A Machine for Measuring the Suspension Characteristics of Agriculture Tyres," *Journal of Terramechanics,* vol. 26, no. 3/4, 1989.

1.38 C.W. Barson, D.H. James, and A.W. Morcombe, "Some Aspects of Tire and Vehicle Vibration Testing," *Proc. Institution of Mechanical Engineers,* vol. 182, part 3B, 1967–1968.

PROBLEMS

1.1 Compare the power required to overcome the rolling resistance of a passenger car weighing 15.57 kN (3500 lb) and having radial-ply tires with that of the same vehicle, but having bias-ply tires in the speed range 40–100 km/h (25–62 mph). The variations of the coefficient of rolling resistance of the radial-ply and bias-ply passenger car tire with speed are described by Eqs. 1.1 and 1.2, respectively.

1.2 A truck tire with vertical load of 24.78 kN (5570 lb) travels on a dry concrete pavement with a peak value of coefficient of road adhesion $\mu_p = 0.80$. The longitudinal stiffness of the tire during braking C_s is 224.64 kN/unit skid (55,000 lb/unit skid). Using the simplified theory described in Section 1.3, plot the relationship between the braking force and the skid of the tire up to skid $i_s = 20\%$.

1.3 Using the simplified theory described in Section 1.4.4, determine the relationship between the cornering force and the slip angle in the range 0–16° of the truck tire described in Problem 1.2. The cornering stiffness of the tire C_α is 132.53 kN/rad (520 lb/deg). Assume that there is no braking torque applied to the tire.

1.4 Determine the available cornering force of the truck tire described in Problems 1.2 and 1.3 as a function of longitudinal skid at a slip angle of 4°, using the simplified theory described in Section 1.4.4. Plot the cornering force of the tire at a slip angle of 4° versus skid in the range 0–40%. The coefficient of road adhesion is 0.8.

1.5 A passenger car travels over a flooded pavement. The inflation pressure of the tires is 179.27 kPa (26 psi). If the initial speed of the car is 100 km/h (62 mph) and brakes are then applied, determine whether or not the vehicle will be hydroplaning.

1.6 An all-terrain vehicle weighs 3.56 kN (800 lb) and has four terra tires, each of which has a vertical stiffness of 52.54 kN/m (300 lb/in.) at an inflation pressure of 27.6 kPa (4 psi), and a stiffness of 96.32 kN/m (550 lb/in.) at a pressure of 68.9 kPa (10 psi). Estimate the fundamental natural frequencies of the vehicle in the vertical direction at the two inflation pressures. The vehicle has no spring suspension.

1.7 Using the Magic Formula described in Section 1.4.4, estimate the cornering force of a car tire at a normal load of 6 kN (1349 lb) with a slip angle of 5°. The values of the empirical coefficients in the Magic Formula for the tire are given in Table 1.6.